

ORIGINAL ARTICLE

Open Access



Study on systematic errors of BDS-3 broadcast ephemeris and their effects with Helmert transformation

Min Li¹, Jiangnan Zhang², Guo Chen^{1*} , Liang Chen³ and Qile Zhao¹

Abstract

Previous studies have not evaluated the systematic errors implied in the third generation of BeiDou-3 Navigation Satellite System (BDS-3) broadcast ephemeris. In this paper we evaluate the systematic pattern described by the Helmert transformation parameters, including translations, rotations, and scale. BDS-3 broadcast and precise ephemerides from December 2019 to 2022 are collected, and the characteristics of the transformation parameters as well as their effects on the signal in space error are analysed. The annual variation in the z-translation is obtained, and the similar amplitudes of 5.5 cm and phases of approximate 300 days are obtained for different years. When the rotation parameters are considered in the orbit comparison, the Root Mean Square (RMS) errors of the along- and cross-track orbital differences decrease from 29.1 to 12.5 cm and from 30.6 to 9.2 cm, respectively, because the three rotation parameters compensate for the majority of the errors in the BDS-3 broadcast ephemeris. Moreover, the high correlations in the obtained rotation parameters among the three orbital planes suggest that the orientation of the BDS-3 broadcast ephemeris is influenced by common model errors, i.e., uncertainty of Earth Rotation Parameters (ERPs). Further research is required because an offset of 1.5×10^{-9} for the scale parameter is observed. A degraded User Range Error (URE) for epochs of up to 84% is attained when the systematic pattern is considered, though the impact of the systematic pattern indicated by the z-translation and rotation parameters on the URE is less than 5.0 cm. With the refinement of the ERPs implemented in the new generation of broadcast ephemeris, we anticipate that the broadcast ephemeris performance of BDS-3 will be improved.

Keywords Broadcast ephemeris, BDS-3, Helmert transformation, Transformation parameters, Correlation coefficient, URE

Introduction

As a new emerging Global Navigation Satellite System (GNSS), the BeiDou Navigation Satellite System (BDS) has completed the development of its third stage. BeiDou-3

Navigation Satellite System (BDS-3), in contrast to BeiDou-2 Navigation Satellite System (BDS-2), which offered services to the users only in the Asia–Pacific region, has been offering global Positioning, Navigation, And Timing (PNT) services since its formal commissioning in December 2018 (Yang et al., 2020). For a standard PNT user, the broadcast ephemerides of GNSS play a crucial role. Consequently, the assessments and monitoring of the Signal in Space Error (SISE) consisting of orbit and clock errors are often conducted by the GNSS community and its control segment.

Compared to the precise products obtained by Wuhan University (WHU), Chen et al. (2013) assessed the

*Correspondence:

Guo Chen

guo_chen@whu.edu.cn

¹ GNSS Research Center, Wuhan University, No. 129 Luoyu Road, Wuhan 430079, China

² School of Geodesy and Geomatics, Wuhan University, No. 129 Luoyu Road, Wuhan 430079, China

³ School of Electronic and Information Engineering, Beihang University, Beijing 100191, China



© The Author(s) 2023. **Open Access** This article is licensed under a Creative Commons Attribution 4.0 International License, which permits use, sharing, adaptation, distribution and reproduction in any medium or format, as long as you give appropriate credit to the original author(s) and the source, provide a link to the Creative Commons licence, and indicate if changes were made. The images or other third party material in this article are included in the article's Creative Commons licence, unless indicated otherwise in a credit line to the material. If material is not included in the article's Creative Commons licence and your intended use is not permitted by statutory regulation or exceeds the permitted use, you will need to obtain permission directly from the copyright holder. To view a copy of this licence, visit <http://creativecommons.org/licenses/by/4.0/>.

broadcast ephemerides of BDS-2 satellites and found the Root Mean Square (RMS) values of orbital differences of 2.1, 1.5, and 1.4 m for the Geostationary Earth Orbit (GEO), Inclined Geo-Synchronous Orbit (IGSO) and Medium Earth Orbit (MEO) satellites of BDS-2. Using one-year ephemerides, the user range errors of the signal in space were assessed by Hu et al. (2013). The average User Range Error (URE) of IGSO was 1.2 m, while the URE of MEO was gradually improved from 3.5 to 1.2 m and the average precision of 5 GEO/5 IGSO/4 MEO was approximately 1.5 m. Wu et al. (2017) also evaluated the performances of BDS-2 satellites based on a long-term ephemeris of approximately 4 years, and the results demonstrated that the broadcast clock dominated the URE. Moreover, relatively large orbit error jitters are found whenever the satellites enter the eclipse season (Wu et al., 2017). Thanks to the advanced Ka-band Inter-Satellite Link (ISL), obvious improvements were achieved for the BDS-3 broadcast ephemerides (Xie et al., 2019; Yang et al., 2017) compared to those of BDS-2. Lv et al. (2020) obtained an orbit-only URE of 0.1 m for the initial 18 BDS-3 MEO satellites by comparing the broadcast and precise ephemerides of 55 days, and a URE of 0.5 m was also obtained considering both the orbit and clock errors. Using another 6-month dataset in 2019, Shi et al. (2020) validated that the orbit and clock uncertainties of BDS-3 MEO satellites were improved from 2.0 m and 2.91 ns for BDS-2 to 0.5 m and 1.82 ns, respectively. A significant improvement in the positioning service with the additional satellites of the BDS-3 preliminary system was also achieved in that study (Shi et al., 2020). Collecting 3-month broadcast ephemerides of the four GNSSs, i.e., Global Positioning System (GPS), GLObal NAVigation Satellite System (GLONASS), BDS-3, and Galileo navigation satellite system (Galileo), in 2019, Montenbruck et al. (2020) assessed and compared the SISEs of the four constellations and reported that Galileo and BDS-3 achieved the smallest UREs of the orbit and clock error budgets.

In the studies mentioned above, the discrepancies in the reference frames were typically ignored when comparing broadcast and precise ephemerides. As a result, the assessment results included inconsistencies among reference frames. It is commonly known that Helmert transformation parameters can be used to explain any systematic discrepancies between two sets of positions in separate terrestrial reference frames (Boucher & Altamimi, 2001; Malys et al., 2021). Chen et al. (2021) estimated rotation parameters based on a Helmert transformation between broadcast and precise ephemerides, and the largest rotations were found for BDS-2 and BDS-3 constellations compared to the other three GNSSs. Moreover, an obvious linear pattern was

noticed in the Satellite Laser Ranging (SLR) residuals of BDS satellites in the same study (Chen et al., 2021), which was related mainly to the solar radiation pressure model adopted in the precise ephemeris determination and prediction method. In another study, Chen et al. (2022a) further validated obvious systematic rotation and translation errors of BDS-3 broadcast ephemerides compared to those of GPS and Galileo, and a similar pattern was also confirmed in precise positioning using broadcast ephemerides.

Benefiting from the improved performance of broadcast ephemerides, especially for the two newest constellations (i.e., Galileo and BDS-3), it is possible to achieve Precise Point Positioning (PPP) at the decimetre accuracy level using broadcast ephemerides without any external information. By compensating the SISE of broadcast ephemerides using a specific parameter in the PPP model, Carlin et al. (2021) achieved a position accuracy of 25 cm for Galileo/GPS integrated kinematic PPP. Although Galileo dominated this positioning accuracy due to its SISE being smaller than that of GPS, the multi-constellation solution is still preferred because it can provide more visible satellites, and robust positioning results can be expected (Bahadur & Nohutcu, 2018; Cai & Gao, 2013). Chen et al. (2022b) validated that integrating BDS-3 into GPS/Galileo PPP with broadcast ephemerides improved the static and kinematic modes by 1 and 5 cm, respectively. With the promising performance of multi-GNSS broadcast ephemerides, a resilient solution can be provided for the future orbit determination of massive Low Earth Orbit (LEO) constellations based on PPP with broadcast ephemerides (Montenbruck et al., 2022a; Wang et al., 2020; Gong et al., 2020). However, the possible systematic errors presented in broadcast ephemerides should be carefully analysed and considered in the application of PPP with broadcast ephemerides.

In this contribution, the Helmert transformation is used to analyse the systematic errors of BDS-3 broadcast ephemerides from the perspective of a relatively long timescale. This article is organized as follows. After the introduction, the collection of the broadcast and precise ephemerides is presented in the section "Data source", and the calculation methods for the assessment of broadcast ephemerides are introduced in the section "Computation of systematic characteristics for BDS-3 broadcast ephemerides". In the section "Results and discussion", the Helmert transformation parameters are analysed in detail within the satellites and orbital planes, as well as the impacts induced by these transformation parameters on the SISE. Finally, the summary and conclusion are given.

Data source

To compute and analyse the transformation parameters between the precise orbits and broadcast ephemerides, the navigation ephemerides from December 2019 to December 2022 were downloaded from the FTP server of the WHU data centre (<ftp://igs.gnsswhu.cn>).

Precise BDS-3 ephemerides are routinely generated by the analysis centres of the International GNSS Service (IGS) Multi-GNSS Pilot Project (MGEX) and International GNSS Monitoring and Assessment System (iGMAS) (Montenbruck et al., 2017; Zhou et al., 2022). The precise products produced by GeoForschungsZentrum (GFZ) were chosen for the orbit comparison herein since the processing strategies are consistent during the test period (Deng et al., 2022). Due to the low-quality and regional limited coverage of the IGSO and GEO satellites of BDS-3, only the MEO satellites were used for the orbit comparison. Precise products were not available for C41-C44 until June 21, 2020, though the corresponding broadcast ephemerides are retrievable. For the other MEO satellites (i.e., C19-C37), the precise orbits are available for the whole period except a few days.

Computation of the systematic characteristics of BDS-3 broadcast ephemerides

In this section, the Helmert transformation is employed to describe the systematic characteristics of BDS-3 broadcast ephemerides, including 3 translations, 3 rotations, and 1 scale. To assess the impacts of the Helmert transformation parameters on the SISE, the URE indicator is also obtained.

Helmert transformation

By assuming the geometric similarity between the reference frames realized by the precise orbit and broadcast ephemerides for the Helmert transformation, the transformation parameters can be calculated as follows:

$$X_{pre}^{apc} = (1 + m) \begin{bmatrix} 1 & R_Z & -R_Y \\ -R_Z & 1 & R_X \\ R_Y & -R_X & 1 \end{bmatrix} X_{brd}^{apc} + T \tag{1}$$

where $T = [T_X \ T_Y \ T_Z]^T$ and $[R_X \ R_Y \ R_Z]^T$ are the translation and rotation vectors, respectively, m is the scale factor, X_{brd}^{apc} and X_{brd}^{apc} are the position vectors of the same satellite derived from the broadcast ephemeris and precise orbit, respectively, expressed in the Earth-Centred-Earth-Fixed (ECEF) coordinate system.

The precise orbit is referenced to the point of Centre of Mass (CoM) and should be transformed to the Antenna Phase Centre (APC) of the satellite to be consistent with that of the broadcast ephemeris. The Phase Centre Offset

(PCO) corrections from the China Satellite Navigation Office (CSNO) are applied to align the reference point of the GFZ precise orbit from CoM to APC as follows:

$$X_{pre}^{APC} = X_{pre}^{CoM} + A^S X_{PCO} \tag{2}$$

where X_{pre}^{APC} and X_{pre}^{CoM} are the precise positions referred to as APC and CoM, respectively, A^S represents the coordinate transformation matrix from the satellite body fixed system to the ECEF, and X_{PCO} is the coordinate of the point of the mean phase centre offset for the satellite, which is generally described in the satellite body-fixed frame.

Considering that the update interval of the BDS-3 broadcast ephemeris is 1 h, Helmert transformation processing is conducted using one epoch of satellite positions for each hour. Generally, 24 sets of transformation parameters are obtained for each day. Moreover, the satellite positions calculated from the broadcast ephemeris are considered outliers if they differ from the precise orbits by more than 3 m. In addition, the epochs with orbit differences 3 times larger than the yearly standard deviation are excluded in the computation of Helmert transformation parameters. Consequently, there are approximately 4,189 epochs, and less than 1% of the total dataset is removed for the test period.

URE

The orbit errors in the radial, along-track, and cross-track directions are calculated for individual satellites to assess the impacts of possible systematic differences between the broadcast and precise orbits on the SISE. The URE of the broadcast ephemeris s_{URE} is also obtained based on the following formula:

$$s_{URE} = \sqrt{w_R^2 R^2 + w_{AC}^2 (A^2 + C^2)} \tag{3}$$

where R , A and C denote the RMS of the broadcast ephemeris in the radial, along-track, and cross-track directions, respectively, and w_R and w_{AC} are the weight factors for the global averaging signal-in-space range error related to a specific satellite and are selected as 0.981 and 0.136, respectively, for the BDS-3 MEO satellites (Montenbruck et al., 2015).

Results and discussion

In this section, the characteristics of the Helmert transformation parameters between the broadcast and precise satellite positions are presented. For the statistics of Helmert transformation parameters, the epochs with

values larger than 3 times the yearly Standard Deviation (STD) are removed.

Transformation parameters

Translation

The daily translation biases and STDs of the BDS-3 broadcast ephemerides are shown in Fig. 1. Although the hourly transformation parameters are prone to be impacted by the accuracy of the broadcast ephemeris, the daily translation biases vary around zero, with averages of -1.3 , -6.0 , and -0.2 mm for T_X, T_Y and T_Z , respectively. The daily STDs are mostly smaller than 100 mm, and their means are 28.3, 50.6 and 23.4 mm for the three components, respectively. Although the z-translation parameter achieves the smallest daily STDs, it shows an obvious annual period, which can be validated by the spectral amplitudes illustrated in Fig. 2. Generally, the T_Z amplitude reaches a maximum value of approximately 10 cm in June and December of each year.

Rodriguez-Solano et al. (2012a, b) demonstrated that the z-component of the GNSS-derived geocentre is prone to be impacted by the Solar Radiation Pressure (SRP) model in orbit determination. Moreover, a systematic linear pattern of SLR residuals with respect to the Sun-elongation angle is illuminated for the precise products of BDS-3 MEO satellites using the five-parameter Extended CODE (Center for Orbit Determination in Europe) Orbit Model (ECOM) and may be further reduced by the updated ECOM model (Zhao et al., 2022). Consequently, we suspect that the annual variations in

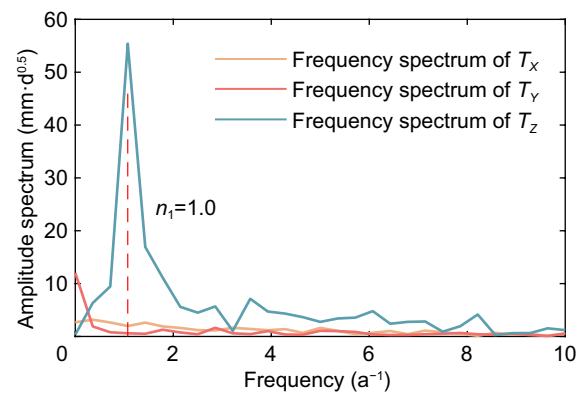


Fig. 2 Periodograms of the translation parameters of the BDS-3 MEO broadcast ephemeris

T_Z may be related to the imperfect SRP model adopted in the generation of the BDS-3 broadcast ephemeris and that the annual amplitude is likely amplified by regional stations (Duan et al., 2022; Zhou et al., 2020).

The systematic pattern in the z-translation can be described by the following function:

$$T_Z = A_Z \sin(w_1 \Delta t + \varphi_{A_Z}) + D_Z \tag{4}$$

where A_Z and φ_{A_Z} are the amplitude and phase, respectively, of the annual signal with a frequency of w_1 .

Figure 3 illustrates the yearly variations in T_Z and the residuals with the fitting function based on Eq. (4), and Table 1 summarizes the coefficients and RMS.

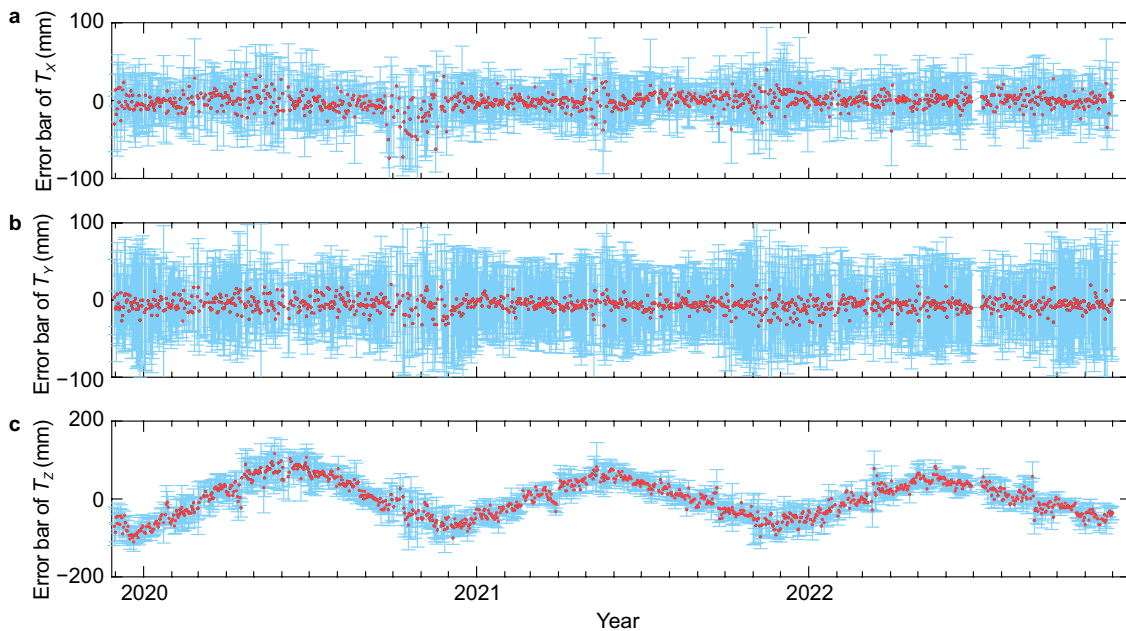


Fig. 1 Daily average and standard deviation values of the x-translation (a), y-translation (b) and z-translation (c) parameters for the BDS-3 MEO broadcast ephemeris compared to precise products

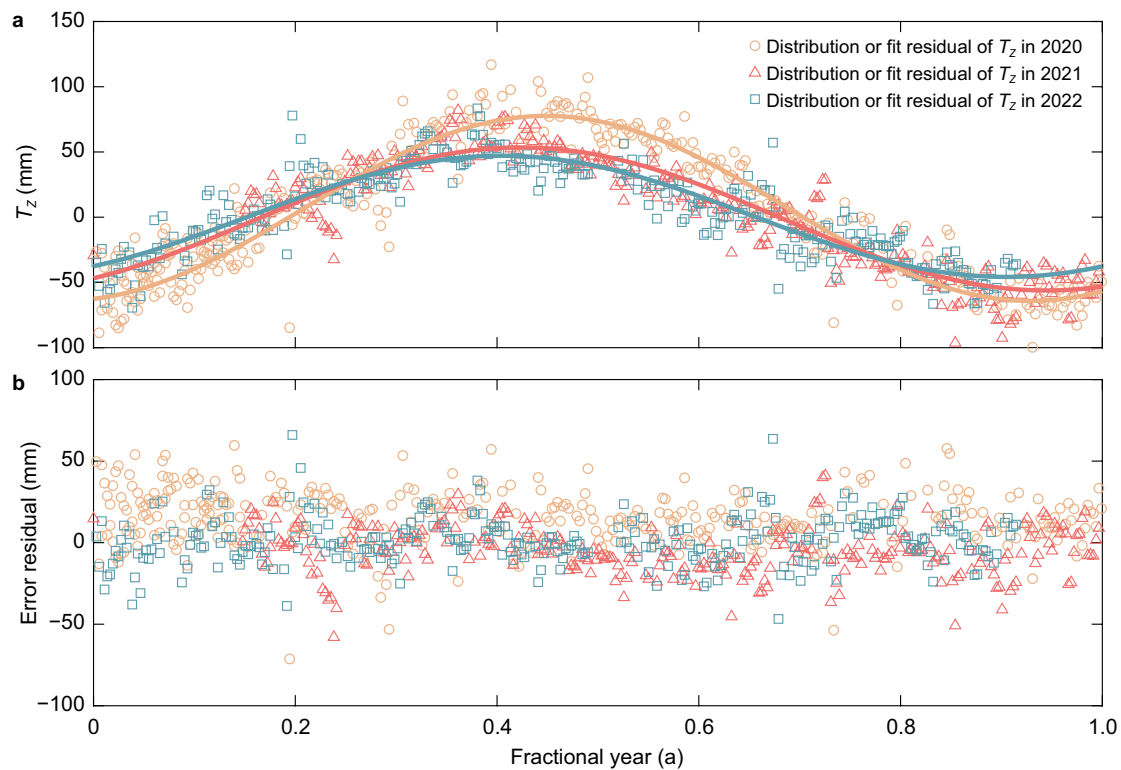


Fig. 3 Daily z-translation (a) and the fitting residuals (b). The lines indicate the fitting results for each year, and the x-axis indicates the fractional year of each year

Table 1 Coefficients of the fitting results for the z-translation

Year	$A_z(\text{mm})$	$\varphi_{A_z}(\text{d})$	$D_z(\text{mm})$	RMS of T_z (mm)	RMS of T_z residuals (mm)
2020	70.9	274.7	6.7	53.8	16.5
2021	54.8	321.7	-1.4	41.0	13.9
2022	46.4	309.5	0.7	34.9	14.7

A similar pattern is found in different years, and the annual phases of different years are almost the same. Nevertheless, there is still some inconsistency in the amplitude of the fitting function. The annual amplitude decreases from 70.9 mm in 2020 to 46.4 mm in 2022, which may be related to the improved performance of the broadcast and/or precise ephemerides.

Once the fitting values are subtracted from the translation T_z , a small RMS of 14–17 mm is achieved for the residuals, indicating that approximately 58–69% of the T_z variations can be described by a systematic pattern using Eq. (4). This finding also means that a similar improvement could be achieved for the precision of the BDS-3 broadcast ephemeris when the annual correction of T_z is considered in orbit assessment.

The transformation parameters are also computed for GPS and Galileo broadcast ephemerides (not shown), and similar annual patterns are found for T_z with amplitudes of 51.8 and 32.3 mm for these two constellations, respectively. This indicates that common SRP errors dominate the variations in T_z for both broadcast ephemerides of different constellations. Arnold et al. (2015) demonstrated that the annual amplitude of the GPS geocentre z-coordinate derived from the 5-parameter ECOM model was two times as large as the result determined by SLR, as the SLR result could be reduced significantly by the updated ECOM with the additional consideration of even-order, short-period harmonic perturbations along the Sun-satellite direction. For the geocentres derived from BDS, Li et al. (2023) illustrated that the a priori box-wing along with the 5-parameter ECOM model can reduce the annual amplitude of the z-coordinate (i.e., 61.1–84.6 mm) by a factor of 2.9.

Scale

Figure 4 displays the scales of the BDS-3 broadcast ephemerides compared to precise products for the years 2020–2022. It is clear that the daily scales fluctuate between 0 and 3×10^{-9} , with a resultant average of 1.48×10^{-9} . Moreover, the daily scales have no apparent

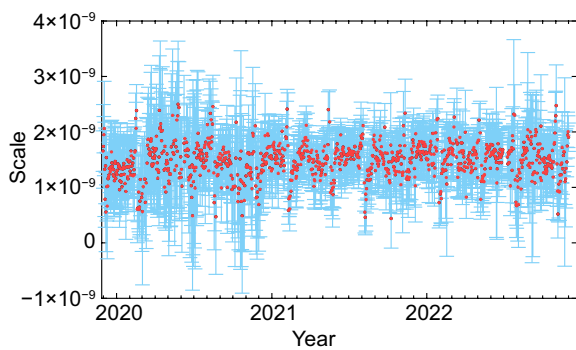


Fig. 4 Daily average and standard deviation of scale parameters for the BDS-3 MEO broadcast ephemerides compared to precise products

offset, indicating that the scale realized by the broadcast ephemerides of new satellites is comparable to that of earlier satellites. Overall, an STD of 0.54×10^{-9} is achieved for the daily scale.

The scale bias can be explained by two factors: first, the scale estimates are strongly correlated with the PCO values adopted for the reference point alignment of the broadcast ephemeris, and any PCO inconsistencies between the broadcast and precise orbits could introduce scale estimation biases (Montenbruck et al., 2022a, 2022b; Zhu et al., 2003); second, the satellite antenna thrust or the Earth albedo perturbation are not considered, and the inconsistency model of these two non-conservative forces could also introduce a radial satellite

orbit bias that could be absorbed by the scale parameter in Helmert transformation. When the antenna thrust is considered in the GNSS orbit determination, the radial orbit bias can reach 2.7 cm (i.e., approximately 1.0×10^{-9}) depending on the transmit power, the satellite mass, and the orbital period (Steigenberger et al., 2018). The Earth albedo, consisting of visible light and infrared emission, can introduce an average bias of radial orbit difference of 1 cm for GPS satellites depending on the geometrical and optical properties of the spacecraft (Rodriguez-Solano et al. 2012a, b). A comparison between BDS-3 orbits with and without the consideration of antenna thrust and Earth albedo shows increases of 3–4 cm in the SLR residual biases (Guo et al., 2023).

Rotation

The rotation parameters are shown in Fig. 5. For the rotations along the x -, y - and z -axis (i.e., R_x , R_y and R_z), the daily rotations fluctuate mostly within ± 5 milli-arcsecond (mAs). The averages of the three-year rotations are 0.460, -0.064 and 0.589 mAs for R_x , R_y and R_z , respectively, and the averages of their daily STDs are 0.760, 0.890 and 0.656 mAs, respectively.

The ranges of the rotation variations for the GPS and Galileo broadcast ephemerides are within ± 2 mAs (not shown), indicating that the relatively large orientation errors are obtained for BDS-3. Since the GNSS technique is unable to determine the orientation of the station-satellite observation network and ERP simultaneously, any ERP bias is compensated by a rotation of the whole

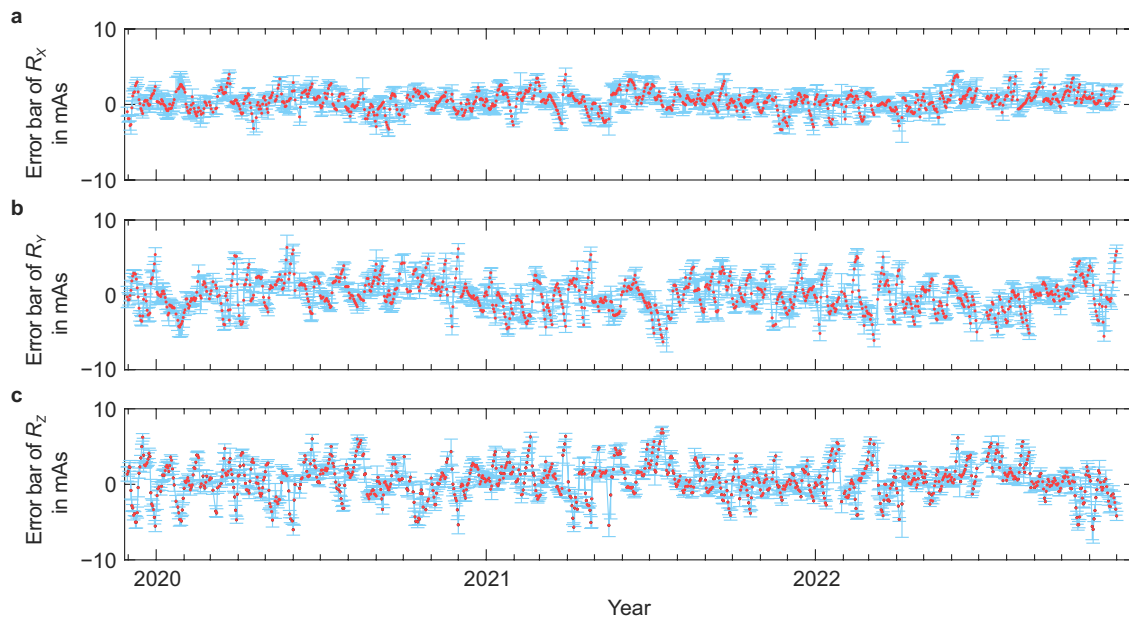


Fig. 5 Daily average and standard deviation values of the x -rotation (a), y -rotation (b) and z -rotation (c) parameters for BDS-3 MEO broadcast ephemerides compared to precise products

constellation, and vice versa. Consequently, the obvious uncertainty of the ERP explains the violent fluctuations in the rotation parameters of the BDS-3 broadcast ephemeris.

A short period is presented in the rotation variations, during which the rotations increase and can reach 20 mAs for RY. Chen et al. (2022a) illustrated that the short period of the rotations was related to the weekly update interval of the ERP used in orbit determination. Figure 6 presents the quantiles (i.e., 2.5, 25, 50, 75, and 97.5%) of the rotation parameters for each day of the week. The range of middle 95% rotations increases from Tuesday of each week in 2020, which is consistent with the results of Chen et al. (2022a). A similar pattern is also found for the rotations in 2021, suggesting that the ERP predictions degrade over time within each week. However, the update epoch differs in 2022, when the ERPs are most likely updated on Thursday.

The broadcast ERPs are gathered and compared to the precise products to verify the effects of the ERP on the BDS-3 broadcast ephemeris. The fluctuations of the broadcast ERP difference (i.e., dX_{pole} , dY_{pole} , and dt_{UT1}) against the rotation parameters are shown in Fig. 7. Despite some jitters far away from the fitting line, a high correlation is found between the rotations and ERP,

especially for the two-pole-motion parameters. The overall correlation coefficients are 0.77, 0.75, and 0.21 for the three rotation parameters against the corresponding ERPs, indicating the high correlation between the rotations and ERP. The small correlation between dt_{UT1} and R_Z is likely related to the fact that any error in dt_{UT1} could be compensated by the ascending node of the satellite in orbit determination.

Correlation analysis between different orbit planes

This section focuses on the correlations of the Helmert transformation parameters among the three orbital planes of MEO satellites. The correlations of translation parameters among different orbital planes are presented in Fig. 8. For the translations in the x and y directions, no significant correlations are found between different orbit planes, and the coefficients are smaller than 0.15. This can be explained by the fact that the T_X and T_Y derived from orbit comparison are dominated by the errors of BDS-3 broadcast ephemerides and presented as white noise for different orbit planes. Due to the annual pattern presented in the T_Z component (Fig. 2), the correlation coefficients of T_Z reached 0.7. This suggests that the system pattern of T_Z is similar in different years (Fig. 3) and consistent in different orbit planes. Moreover, the high

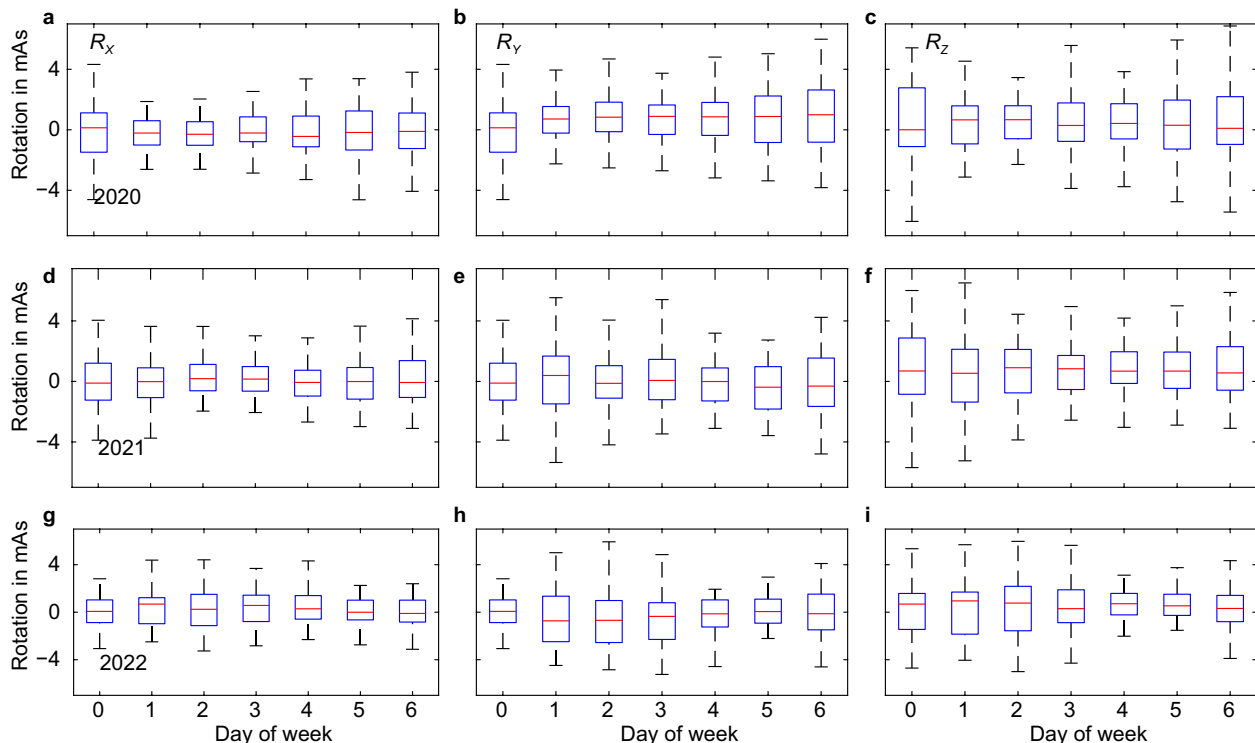


Fig. 6 Quantiles of BDS-3 rotation parameters for each day of the week. The box plot is constructed from the 2.5th, 25th, 50th, 75th, and 97.5th percentiles. These subgraphs show the x-rotation in 2020 (a), 2021 (d) and 2022 (g); the y-rotation in 2020 (b), 2021 (e) and 2022 (h); and the z-rotation in 2020 (c), 2021 (f) and 2022 (i)

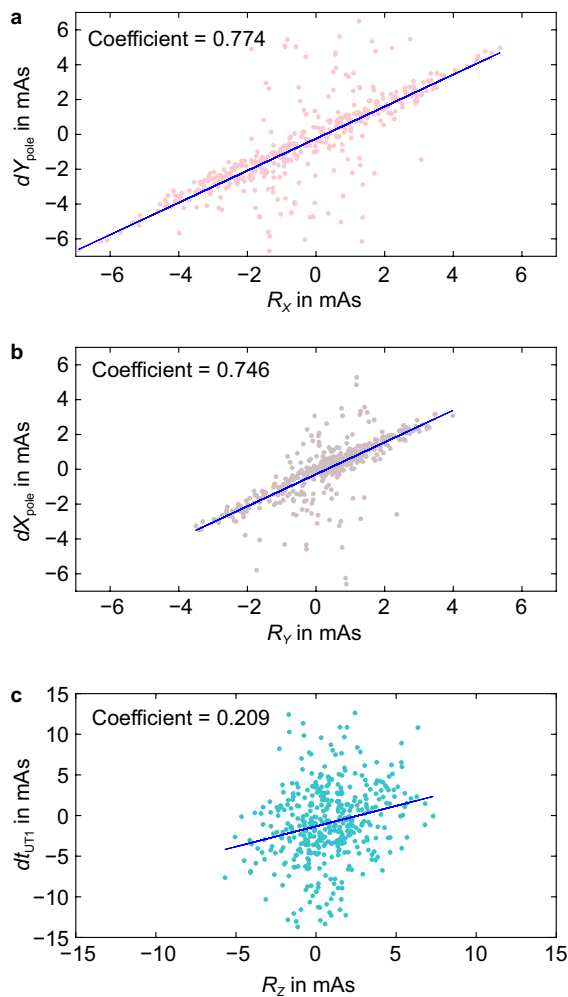


Fig. 7 Correlations between the rotation parameters and ERP differences. The subgraphs show the correlations between the dY_{pole} and x-rotation (a), dX_{pole} and y-rotation (b), and dt_{UTC} and z-rotation (c)

correlations found in different orbit planes indicate that there are common unmodelled effects in the generation of broadcast ephemerides.

Figure 9 demonstrates the correlations of rotations among different orbit planes. A significant correlation within orbit planes is noticed for all three components of the rotation parameters, and correlation coefficients of up to 0.99 are obtained. This indicates that the rotation errors of the BDS-3 broadcast ephemeris are consistent among different orbit planes and related to the whole constellation (i.e., the uncertainty of ERP adopted for the generation of the broadcast ephemeris). Considering that the ERPs are highly correlated to the orientation of the orbit, any deficiency in the ERPs could induce rotation errors in the spatial realization of the terrestrial reference frame (i.e., the satellite orbits). Moreover, larger BDS-3

broadcast ERP errors were found by Steigenberger et al. (2022) compared to the broadcast ERP errors of GPS.

Figure 10 presents a comparison of the scale parameters for different orbital planes. No obvious correlation is found among the three planes, and the parameters are dominated by the scale uncertainty estimated from the orbit comparison. The correlation coefficients do not exceed 0.3. Moreover, a small inconsistency is noticed for the orbital plane scales, and the largest scale offset of 1.82×10^{-9} is obtained for plane B. The smallest offset of 1.16×10^{-9} is found for plane C, and the average scale is 1.43×10^{-9} for plane A. These results can be related to inconsistent antenna thrust and Earth albedo models introducing different radial offsets compared to those of precise products.

Impact on SISE

Without considering the systematic pattern of the BDS-3 broadcast ephemeris, the performance of BDS-3 positioning will deteriorate. In this section, the impacts on the BDS-3 SISE for the systematic pattern described by the transformation parameters are analysed. Due to the obvious annual pattern presented in the z-translation, which can be described by Eq. (4), and the high correlations among different orbital planes for T_z and rotations (Figs. 8 and 9), we will focus on the correction of the T_z and three rotation parameters.

Figure 11 shows the assessments of broadcast ephemerides with and without considering the T_z and rotation corrections for individual MEO satellites (denoted as W_RT and WO, respectively). For a comparison, the results of the broadcast ephemerides corrected with T_z using Eq. (4), and rotations, denoted as W_T and W_R, are also presented separately. Overall, the T_z correction manifests in the radial and along-track components of the broadcast ephemerides, and the mean decreases in RMS are 0.004 and 0.002 m, respectively. The RMS reduction of three dimensions (3D) for W_T is small (i.e., 0.42%) compared to that of WO. However, this does not mean that the T_z correction can be ignored. The periodic pattern for a T_z amplitude reaching one decimetre (i.e., the middle and end of each year) should be compensated in PPP based on the BDS-3 broadcast ephemeris (Chen et al., 2022b).

A pronounced decrease in RMS is obtained for the broadcast ephemerides when the whole constellation rotation is corrected (i.e., W_R) compared to the W_T results. The RMS in the along-track direction is reduced from 0.291 to 0.125 m, and that in the cross-track direction is reduced from 0.306 to 0.092 m. Moreover, the precision improvements are consistent among different satellites, and this is likely related to the high correlations of the rotations among different orbital planes (Fig. 9).

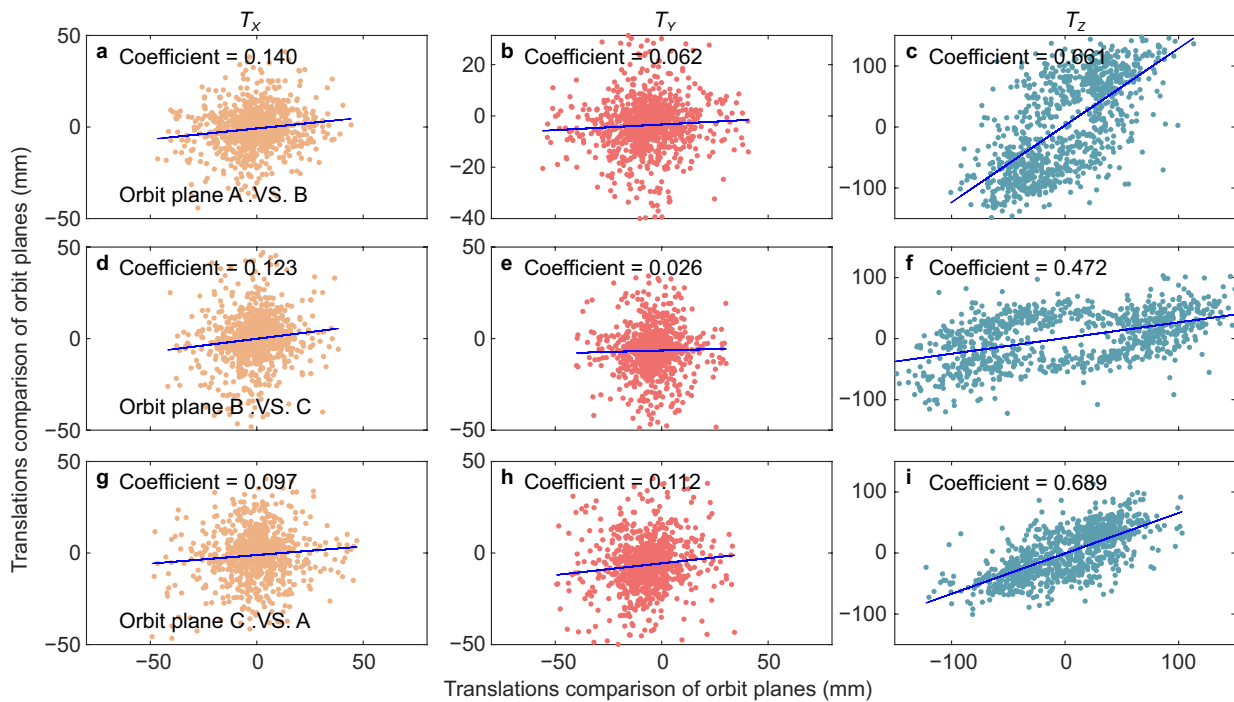


Fig. 8 Correlations of translation parameters among orbital planes. The subgraphs show the correlations of the x-translation between orbit planes A and B (a), B and C (d), and C and A (g), the correlations of the y-translation between orbit planes A and B (b), B and C (e), and C and A (h), and the correlations of the z-translation between orbit planes A and B (c), B and C (f), and C and A (i)

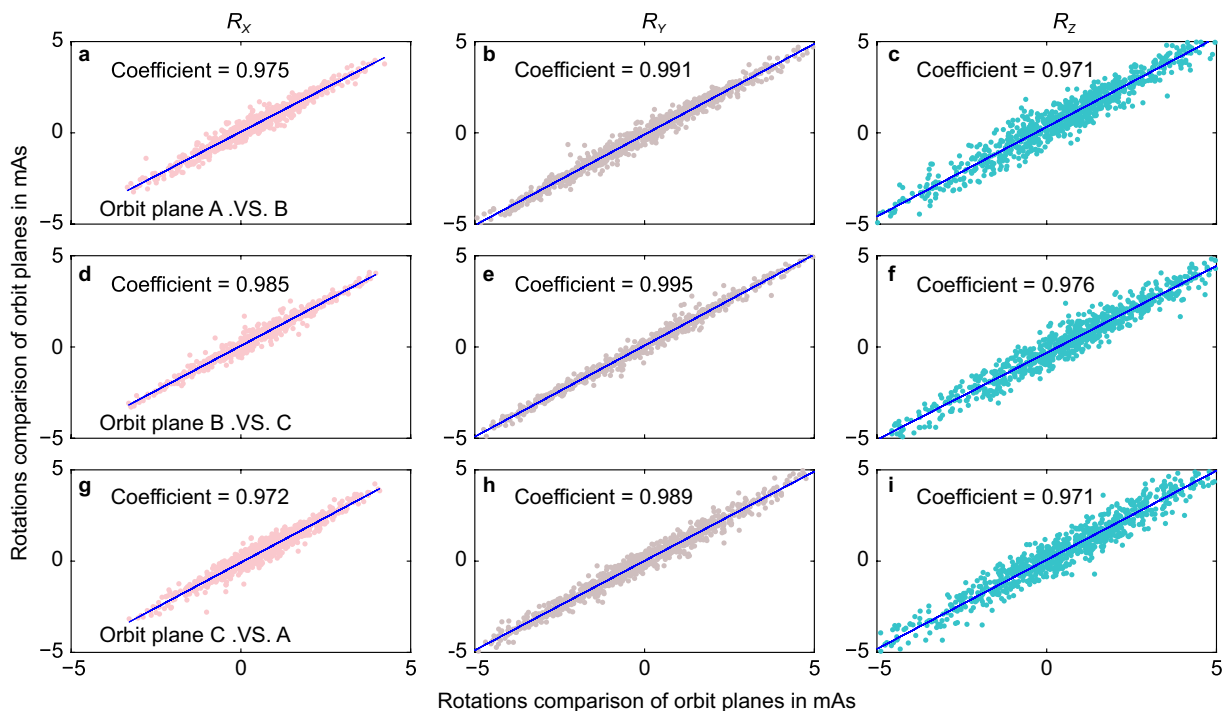


Fig. 9 Correlations of rotation parameters among different orbital planes. The subgraphs show the correlations of the x-rotation between orbit planes A and B (a), B and C (d), and C and A (g); the correlations of the y-rotation between orbit planes A and B (b), B and C (e), and C and A (h); and the correlations of the z-rotation between orbit planes A and B (c), B and C (f), and C and A (i)

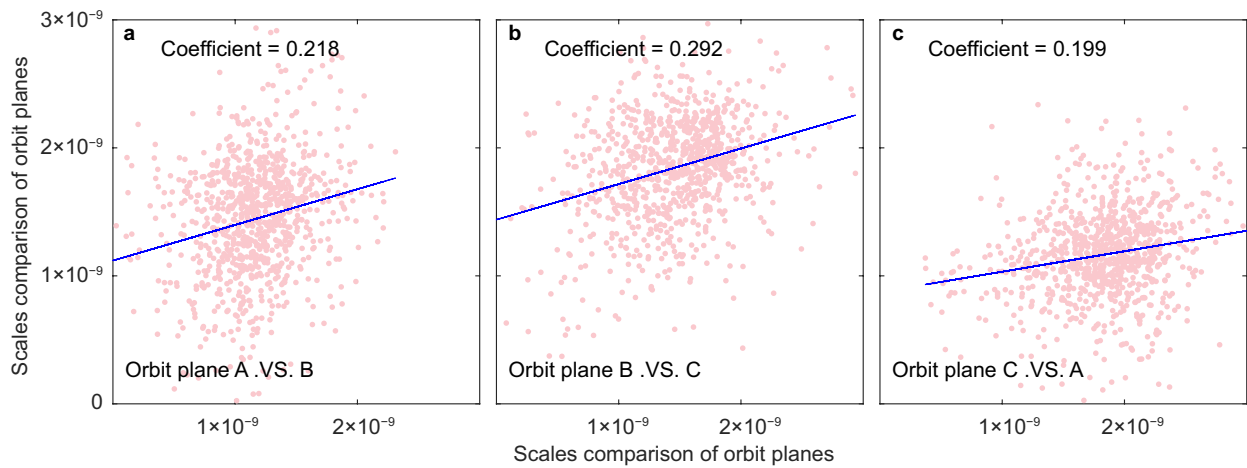


Fig. 10 Correlations of the scale parameters among different orbital planes. The subgraphs show the scale correlations between orbit planes A and B (a), B and C (b), and C and A (c)

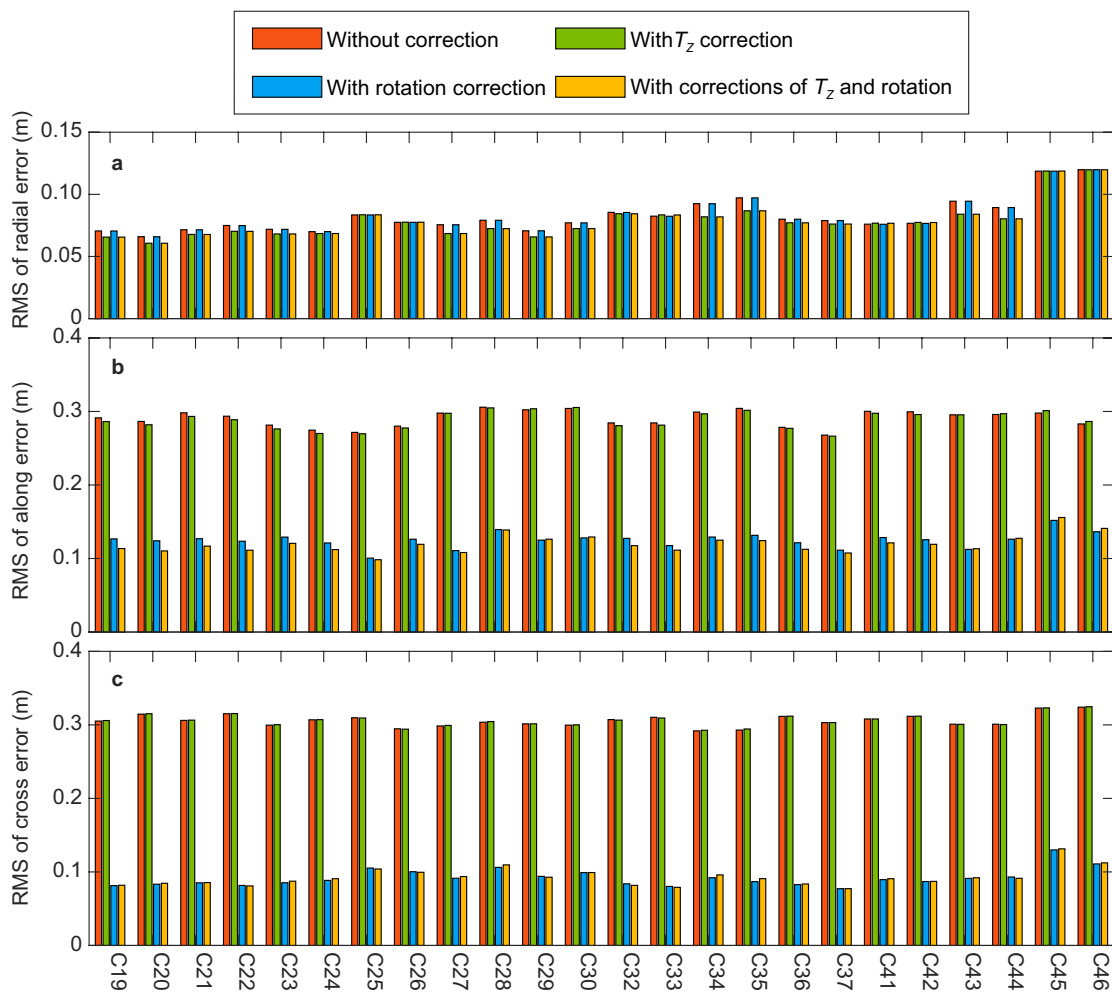


Fig. 11 RMS values of individual BDS-3 MEO satellites with and without consideration of the z-translation and rotation corrections in the radial (a), along-track (b) and cross-track (c) directions

Because the rotation errors do not act on the radial direction, there is no decrease in RMS in this direction. Considering both T_Z and the rotations for the broadcast ephemeris assessment, the RMS is further decreased for W_RT compared to W_R. The average 3D RMS values obtained for the BDS-3 MEO satellites are 0.430, 0.428, 0.176 and 0.171 m for WO, W_T, W_R and W_RT, respectively.

To evaluate the effects of the T_Z and rotations on the SISE, the orbit-only URE is used. The changes in URE between the broadcast ephemerides with and without z-translation and/or rotation corrections are shown in Fig. 12. A negative difference means a smaller URE is obtained for the orbits when the systematic pattern is considered. Once again, a pattern similar to URE differences among different satellites is observed, suggesting a

common type of the defect implied in the BDS-3 broadcast ephemeris. Additionally, this finding implies that there are obvious error sources dominating the performance of the broadcast ephemerides, such as the deficiencies in the ERP and SRP models.

Figure 13 shows the distribution of the orbit-only URE differences of all satellites. A decreased URE of broadcast ephemerides with z-translation and rotation corrections is achieved compared to the results obtained without any corrections. The UREs of 65.8% epochs, 82.6% and 84.3% epochs decrease for the broadcast ephemeris with the compensation of z-translation, rotation and the combined errors, respectively. Since the orbit errors in the along- and cross-track directions have limited effects on the URE (i.e., 0.136) based on Eq. (3), the amplitude of the URE difference induced by the rotation errors in the

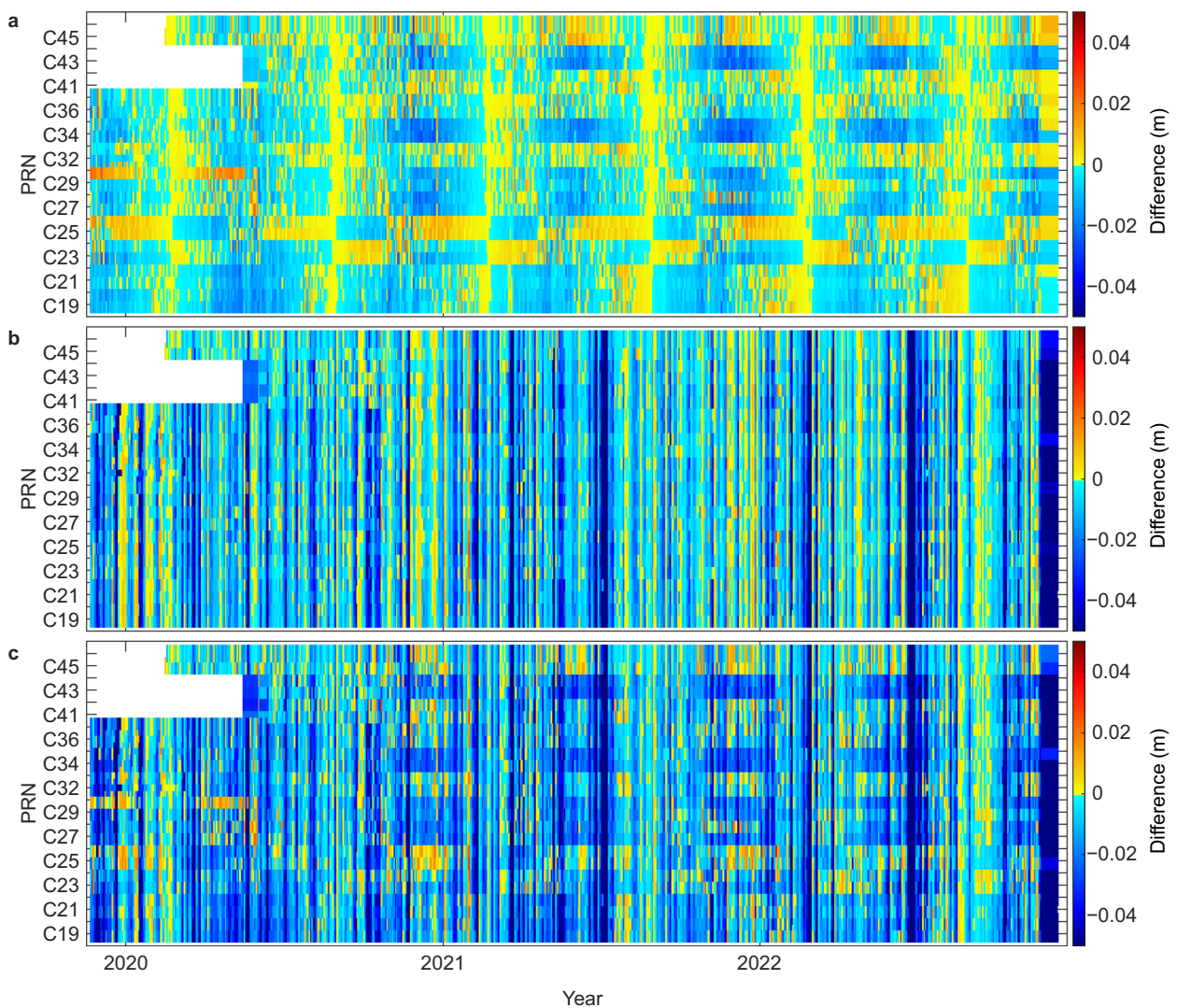


Fig. 12 Orbit-only URE differences between the broadcast ephemeris with and without the z-translation (a), rotation (b), and z-translation/rotation (c) corrections

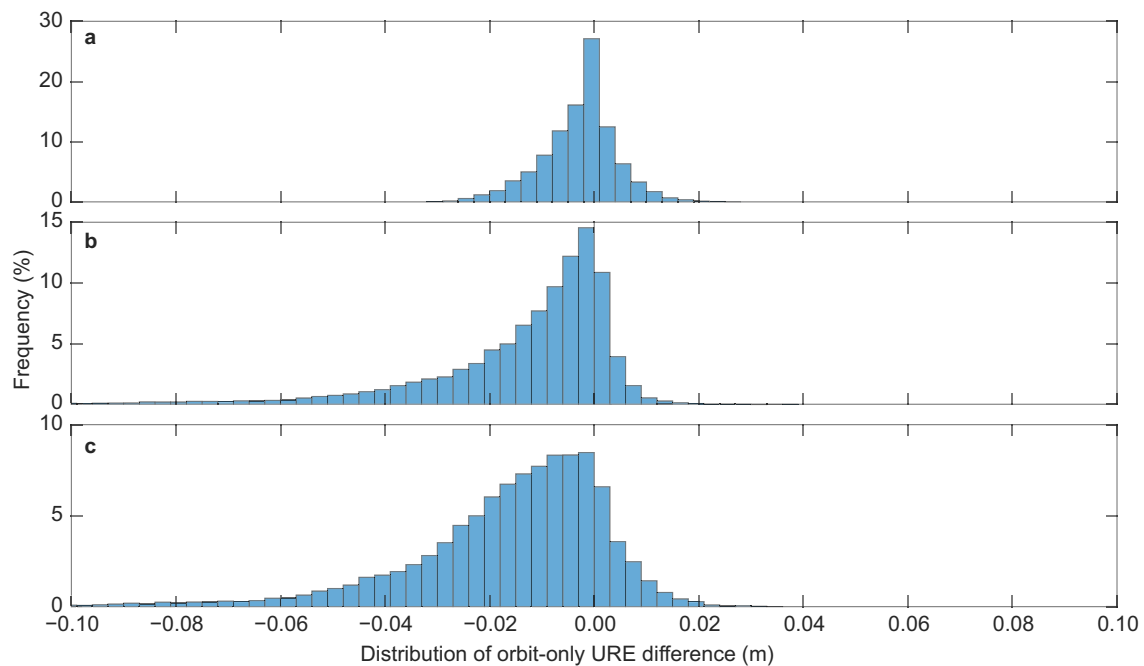


Fig. 13 Distribution of the orbit-only URE difference between the broadcast ephemerides with and without the z-translation (a), rotation (b), and z-translation/rotation (c) corrections

broadcast ephemeris is approximately 1 cm. However, the rotation errors of the whole constellation could still introduce a horizontal positioning bias, as validated by Chen et al. (2022b). A URE difference of up to 3 cm could be induced by the amplitude of the z-translation, and this value is time-dependent (Fig. 12).

Conclusions

The systematic errors of BDS-3 broadcast ephemeris over three years are analysed using the Helmert transformation parameters compared to precise orbits. The characteristics of translation, rotation and scale parameters derived from the orbit comparison are first analysed. Afterwards, the correlations among different orbital planes are assessed to examine the transformation parameters. Finally, the impacts of the translation and rotation errors implied in the broadcast ephemeris on the SISE are illuminated.

Although the transformation parameters derived herein are affected by the uncertainty of the broadcast ephemeris, similar annual z-translation characteristics are found in different years. The z-translation fluctuation can be effectively described as an annual periodic function, and an RMS decrease by 60% is achieved when the systematic pattern is subtracted from the z-translation by the obtained function. The BDS-3 broadcast ephemeris is also much affected by rotation errors of the whole constellation, and the RMS values of the along-track and

cross-track components can be reduced from 29.1 and 30.6 to 12.5 cm and 9.2 cm, respectively, when the rotation parameters are considered in the orbit comparison. Moreover, small weekly increases in rotation errors are noticed for the three-year broadcast ephemerides and are likely related to the ERP updates associated with the orbit determination and prediction. Regarding the scale parameter, an offset of 1.5×10^{-9} is found for the BDS-3 broadcast ephemeris compared to the precise orbits and can be explained mainly by the inconsistent antenna thrust and Earth albedo model adopted by the broadcast and precise ephemerides, though further study is needed.

High corrections of up to 0.99 are noticed for the rotations obtained from different orbital planes, suggesting again that the orientations of the broadcast ephemerides of satellites located in different orbital planes are influenced by a common mode error (e.g., the ERP uncertainty). A moderate correlation of 0.6 is also found for the z-translation parameters estimated from different orbital planes, and this was likely induced mainly by the SRP model and amplified by the regional stations applied for the determination of the broadcast ephemerides. Although the z-translation and rotations have decimetre amplitudes, the effects of these systematic patterns on the URE are less than 5.0 cm. To improve the performance of the BDS-3 broadcast ephemeris, further research should be conducted to refine the SRP and ERP.

Acknowledgements

We are grateful to IGS for providing the broadcast navigation files, and to GFZ for providing multi-GNSS precise products.

Author contributions

All the authors contributed to the design of this study. ML and QZ came up with the idea. JZ processed the evaluation of broadcast ephemeris, generated the results and wrote the draft. JZ and GC revised the manuscript, and carried out the data edit. All authors read and approved the final manuscript.

Funding

This study is sponsored by the National Natural Science Foundation of China (42204019, 42030109) and the Key Research and Development Plan Project of Hubei Province (grant number 2020BIB006), Young Elite Scientists Sponsorship Program by CAST (YESS20200308) and Beijing Nova Program (Z211100002121068).

Availability of data and materials

The BDS-3 broadcast ephemerides are openly available by an anonymous user via <ftp://igs.gnsswhu.cn>. The multi-GNSS precise products of GFZ are downloaded from <ftp://ftp.gfz-potsdam.de>.

Competing interests

The authors declare that no conflicts of interest associated with this publication.

Received: 26 December 2022 Accepted: 10 May 2023

Published online: 12 June 2023

References

- Arnold, D., Meindl, M., Beutler, G., Dach, R., Schaer, S., Lutz, S., Prange, L., Sošnica, K., Mervart, L., & Jäggi, A. (2015). CODE's new solar radiation pressure model for GNSS orbit determination. *Journal of Geodesy*, *89*, 775–791. <https://doi.org/10.1007/s00190-015-0814-4>
- Bahadur, B., & Nohutcu, M. (2018). PPPH: A MATLAB-based software for multi-GNSS precise point positioning analysis. *GPS Solutions*. <https://doi.org/10.1007/s10291-018-0777-z>
- Boucher, C., & Altamimi, Z. (2001). ITRS, PZ-90 and WGS 84: Current realizations and the related transformation parameters. *Journal of Geodesy*, *75*, 613–619. <https://doi.org/10.1007/s001900100208>
- Cai, C., & Gao, Y. (2013). Modelling and assessment of combined GPS/ GLO-NASS precise point positioning. *GPS Solutions*, *17*(2), 2236. <https://doi.org/10.1007/s10291-012-0273-9>
- Carlin, L., Hauschild, A., & Montenbruck, O. (2021). Precise point positioning with GPS and Galileo broadcast ephemerides. *GPS Solutions*. <https://doi.org/10.1007/s10291-021-01111-4>
- Chen, G. (2019). Research on the methods for multi-GNSS products combination and its application in iGMAS activities. PhD Dissertation, Wuhan University.
- Chen, G., Wei, N., Li, M., Zhao, Q., Niu, Y., Cai, H., & Meng, Y. (2022a). Assessment of BDS-3 terrestrial reference frame realized by broadcast ephemeris: Comparison with GPS/Galileo. *GPS Solutions*, *26*(1), 18. <https://doi.org/10.1007/s10291-021-01204-0>
- Chen, G., Wei, N., Li, M., Zhao, Q., & Zhang, J. (2022b). BDS-3 and GPS/Galileo integrated PPP using broadcast ephemerides. *GPS Solutions*, *26*(4), 129. <https://doi.org/10.1007/s10291-022-01311-6>
- Chen, G., Zhou, R., Hu, Z., Lv, Y., Wei, N., & Zhao, Q. (2021). Statistical characterization of the signal-in-space errors of the BDS: A comparison between BDS-2 and BDS-3. *GPS Solutions*, *25*(3), 112. <https://doi.org/10.1007/s10291-021-01150-x>
- Chen, L., Jiao, W., Huang, X., Geng, C., Ai, L., Lu, L., & Hu, Z. (2013). Study on signal-in-space errors calculation method and statistical characterization of BeiDou navigation satellite system. In *Proceedings of China satellite navigation conference (CSNC) Lecture notes in electrical engineering 243* (pp 423–434). Springer. https://doi.org/10.1007/978-3-642-37398-5_39
- Deng, Z., Wang, J., & Ge, M. (2022). The GBM rapid product and the improvement from undifferenced ambiguity resolution. *Acta Geodaetica Et Cartographica Sinica*, *51*(4), 544. <https://doi.org/10.11947/j.AGCS.2022.20220022>
- Duan, B., Hugentobler, U., Selmke, I., Marz, S., Killian, M., & Rott, M. (2022). BeiDou satellite radiation force models for precise orbit determination and geodetic applications. *IEEE Transactions on Aerospace and Electronic Systems*, *58*(4), 2823–2836.
- Gong, X., Sang, J., Wang, F., & Li, X. (2020). LEO onboard real time orbit determination using GPS/BDS data with an optimal stochastic model. *Remote Sensing*, *12*(20), 3458. <https://doi.org/10.3390/rs12203458>
- Guo, J., Wang, C., Chen, G., Xu, X., & Zhao, Q. (2023). BDS-3 precise orbit and clock solution at Wuhan University: Status and improvement. *Journal of Geodesy*, *97*, 15. <https://doi.org/10.1007/s00190-023-01705-5>
- Hu, Z., Chen, G., Zhang, Q., Guo, J., Su, X., Li, X., Zhao, Q., & Liu, J. (2013). An initial evaluation about BDS navigation message accuracy. In *Proceedings of China satellite navigation conference (CSNC) 2013. Lecture notes in electrical engineering 243* (pp. 479–491). Springer. https://doi.org/10.1007/978-3-642-37398-5_44
- Li, X., Huang, S., Yuan, Y., Zhang, K., & Lou, J. (2023). Geocenter motions derived from BDS observations: Effects of the solar radiation pressure model and constellation configuration. *Remote Sensing*, *15*(5), 1243. <https://doi.org/10.3390/rs15051243>
- Lv, Y., Geng, T., Zhao, Q., Xie, X., & Zhou, R. (2020). Initial assessment of BDS-3 preliminary system signal-in-space range error. *GPS Solutions*, *24*(1), 16. <https://doi.org/10.1007/s10291-019-0928-x>
- Malys, S., Solomon, R., Drotar, J., Kawakami, T., & Johnson, T. (2021). Compatibility of terrestrial reference frames used in GNSS broadcast messages during an 8 week period of 2019. *Advances in Space Research*, *67*(2), 834–844. <https://doi.org/10.1016/j.asr.2020.11.029>
- Montenbruck, O., & Ramos-Bosch, P. (2008). Precision real-time navigation of LEO satellites using global positioning system measurements. *GPS Solutions*, *12*(3), 187–198. <https://doi.org/10.1007/s10291-007-0080-x>
- Montenbruck, O., Kunzi, F., & Hauschild, A. (2022a). Performance assessment of GNSS-based real-time navigation for the Sentinel-6 spacecraft. *GPS Solutions*, *26*, 12. <https://doi.org/10.1007/s10291-021-01198-9>
- Montenbruck, O., Steigenberger, P., & Hauschild, A. (2020). Comparing the 'Big 4' – a user's view on GNSS performance. In *2020 IEEE/ION position, location and navigation symposium (PLANS)*, April 20–23, 2020, Portland, OR
- Montenbruck, O., Steigenberger, P., & Hauschild, A. (2015). Broadcast versus precise ephemerides: A multi-GNSS perspective. *GPS Solutions*, *19*, 321–333. <https://doi.org/10.1007/s10291-014-0390-8>
- Montenbruck, O., Steigenberger, P., Prange, L., Deng, Z., Zhao, Q., Perosanz, F., Romero, I., Noll, C., Stürze, A., Weber, G., Schmid, R., MacLeod, K., & Schaer, S. (2017). The Multi-GNSS Experiment (MGEX) of the International GNSS Service (IGS)—Achievements, prospects and challenges. *Advances in Space Research*, *59*(7), 1671–1697. <https://doi.org/10.1016/j.asr.2017.01.011>
- Montenbruck, O., Steigenberger, P., Villiger, A., & Rebischung, P. (2022b). On the relation of GNSS phase center offsets and the terrestrial reference frame scale: A semi-analytical analysis. *Journal of Geodesy*, *96*, 90. <https://doi.org/10.1007/s00190-022-01678-x>
- Rodriguez-Solano, C., Hugentobler, U., Steigenberger, P., & Fritsche, M. (2012a). *Impact of solar radiation pressure modeling on GNSS-derived geocenter motion*. EGU 2012, Vienna, Austria
- Rodriguez-Solano, C., Hugentobler, U., & Steigenberger, P. (2012b). Impact of Albedo Radiation on GPS Satellites. In Kenyon, S., Pacino, M., Marti, U. (Eds.) *Geodesy for Planet Earth. International Association of Geodesy Symposium* (Vol. 136). Springer. https://doi.org/10.1007/978-3-642-20338-1_14
- Shi, J., Ouyang, C., Huang, Y., & Peng, W. (2020). Assessment of BDS-3 global positioning service: Ephemeris, SPP, PPP, RTK, and new signal. *GPS Solutions*, *24*, 81. <https://doi.org/10.1007/s10291-020-00995-y>
- Steigenberger, P., Montenbruck, O., Bradke, M., Ramatschi, M., & Hessel, U. (2022). Evaluation of earth rotation parameters from modernized GNSS navigation messages. *GPS Solutions*. <https://doi.org/10.1007/s10291-022-01232-4>
- Steigenberger, P., Thöelert, S., & Montenbruck, O. (2018). GNSS satellite transmit power and its impact on orbit determination. *Journal of Geodesy*, *92*, 609–624. <https://doi.org/10.1007/s00190-017-1082-2>
- Wang, F., Ling, S., Gong, X., & Guo, L. (2020). Decimeter-level orbit determination for FY3C satellite based on space-borne GPS/BDS measurements. *Geomatics and Information Science of Wuhan University*, *45*(1), 810–821. <https://doi.org/10.1303/j.whugis.20180385>

- Wu, Y., Liu, X., Liu, W., Ren, J., Lou, Y., Dai, X., & Fang, X. (2017). Long-term behavior and statistical characterization of BeiDou signal-in-space errors. *GPS Solutions*, 21(4), 1907–1922. <https://doi.org/10.1007/s10291-017-0663-0>
- Xie, X., Geng, T., Zhao, Q., Cai, H., Zhang, F., Wang, X., & Meng, Y. (2019). Precise orbit determination for BDS-3 satellites using satellite-ground and inter-satellite link observations. *GPS Solutions*, 23(2), 40. <https://doi.org/10.1007/s10291-019-0823-5>
- Yang, D., Yang, J., Li, G., Zhou, Y., & Tang, C. (2017). Globalization highlight: Orbit determination using BeiDou inter-satellite ranging measurements. *GPS Solutions*, 21(3), 1395–1404. <https://doi.org/10.1007/s10291-017-0626-5>
- Yang, Y., Mao, Y., & Sun, B. (2020). Basic performance and future developments of BeiDou global navigation satellite system. *Satellite Navigation*, 1, 1. <https://doi.org/10.1186/s43020-019-0006-0>
- Zhao, Q., Guo, J., Wang, C., Lyu, Y., Xu, X., Yang, C., & Li, J. (2022). Precise orbit determination for BDS satellites. *Satellite Navigation*, 3(2), 1. <https://doi.org/10.1186/s43020-021-00062-y>
- Zhou, S., Hu, X., Liu, L., He, F., Tang, C., & Pang, J. (2020). Status of satellite orbit determination and time synchronization technology for global navigation satellite system. *Chinese Astronomy and Astrophysics*, 44(1), 105–118. <https://doi.org/10.1016/j.chinastron.2020.04.007>
- Zhou, W., Cai, H., Chen, G., Jiao, W., He, Q., & Yang, Y. (2022). Multi-GNSS combined orbit and clock solutions at iGMAS. *Sensors*.
- Zhu, S. Y., Massmann, F.-H., & YuY, ReigberC. (2003). Satellite antenna phase center offsets and scale errors in gps solutions. *Journal of Geodesy*, 76(11), 668–672.

Publisher's Note

Springer Nature remains neutral with regard to jurisdictional claims in published maps and institutional affiliations.

Submit your manuscript to a SpringerOpen[®] journal and benefit from:

- ▶ Convenient online submission
- ▶ Rigorous peer review
- ▶ Open access: articles freely available online
- ▶ High visibility within the field
- ▶ Retaining the copyright to your article

Submit your next manuscript at ▶ [springeropen.com](https://www.springeropen.com)
